

Stability loss of the PZT/Metal/PZT sandwich circular plate-disc under “open-circuit” condition

Fazile I. Jafarova · Orujali A. Rzayev

Received: 11.07.2016 / Revised: 14.09.2016 / Accepted: 16.11.2016

Abstract. *The axisymmetric stability loss of the PZT/Metal/PZT sandwich circular plate is investigated. It is assumed that on the lateral-boundary cylindrical surfaces of the piezoelectric face layers the “short-circuit”, however on upper and lower face planes of these layers the “open-circuit” conditions satisfy. The investigations are made by utilizing the so-called three-dimensional linearized theory of stability of the deformable electro-mechanical systems within the scope of the piecewise homogeneous body model. For solution to the corresponding eigenvalue problem the FEM is employed and numerical results on the critical radial compressional stresses acting in the layers of the plate are presented and discussed. These results are obtained for various piezoelectric face and metal core layers and the main attention is focused on the influence of the piezoelectricity on the values of the compressional critical stress. In particular, it is established that the piezoelectricity of the face layer material causes an increase in the values of the critical compressional stress acting in the facepiezoelectric layers.*

Keywords. Piezoelectric material · circular sandwich plate · stability loss · critical stress

Mathematics Subject Classification (2010): 74H55

1 Introduction

The study of the stability loss problems of layered plates and beams containing the layers made of piezoelectric materials (shortly PZT) has attracted the attention of many researchers such as Yang (1998), Jerom and Ganesan (2010) and many others listed therein. In these investigations it was established that the piezoelectricity of the plate or beam materials causes an increase in the values of the mechanical critical forces.

We here consider a brief review of the related recent investigations and begin this review with the paper by Wu and Ding (2015) in which static analysis of the simply supported rectangular plate made of functionally graded piezoelectric material is studied with the use of the refined plate theories. The open- and closed-circuit conditions on the upper and lower face surfaces are considered. The paper by Arefi and Allam (2015) studies the response of the bi-layered circular plate made of functionally-graded piezoelectric material and resting on a Winkler-Pasternak foundation.

The paper by Jabbari et al. (2013) studies the buckling of the sandwich circular plate with piezoelectric face and porous middle layers under radial compression within the scope of the Kirchhoff-Love plate theory. The analytical expression for the critical force is obtained and according to this expression the influence of the problem parameters, as well as of the piezoelectricity of the covering layer material is determined. Note that the results obtained in this paper are acceptable for very thin plates.

As follows from the foregoing brief review that all the foregoing investigations have been made within the scope of the approximate plate theories, the accuracy of which depends significantly on the geometrical and electro-mechanical properties. Consequently, the order of the accuracy of these results can be estimated with the use of the corresponding results obtained within the scope of the 3D exact theories. For instance, the accuracy of the results related to the stability loss or buckling delamination problems can be estimated with the corresponding results obtained within the scope of the 3D exact linearized theories, the present level of which has been detailed in the monograph by Guz (1999) who made many fundamental contributions to creating this theory. Note that the 3D linearized stability loss theories for the elements of constructions made of time-dependent materials was developed in the monograph by Akbarov (2013).

In the foregoing sense, the first attempt with respect to the stability loss problems related to the system comprising elastic and piezoelectric constituents was made in the paper by Akbarov and Yahnioğlu (2013). Consequently, the study of stability loss of elements of constructions made of piezoelectric materials by employing 3D linearized stability loss theories is in its starting position.

Taking the foregoing situation into consideration in the present paper the study of the 3D stability loss problems for the layered plates made of piezoelectric and metal materials is developed and the axisymmetric stability loss of the circular sandwich PZT/Metal/PZT plate is investigated under compression of that in the radial inward direction by uniformly distributed rotationally symmetric forces.

Note that the corresponding problems for the case where the circular plate consists of elastic and viscoelastic constituents are made in the papers by Akbarov and Rzayev (2002) and Rzayev and Akbarov (2002) the results of which are also detailed in the monograph by Akbarov (2013).

2 Formulation of the problem.

Consider a circular sandwich plate whose geometry is shown in Fig. 1 and for generality, assume that the materials of all the layers are piezoelectric ones. We suppose that the materials of the upper and lower face planes are the same.

We associate with the lower face layer of the plate the cylindrical coordinate system $O r \theta z$ (Fig. 1) and the position of the points of the plate we determine through the Lagrange coordinates in this system. Thus, according to Fig. 1, in the selected coordinate system, the plate occupies the region $\{0 \leq r \leq \ell/2; 0 \leq \theta \leq 2\pi; 0 \leq z \leq h\}$.

Thus, within the framework of the foregoing assumptions, we suppose that the plate is compressed in the inward radial direction by uniformly distributed rotationally symmetric normal forces with intensity p acting on the lateral surface of the circular plate-disc. Below

we will denote the values related to the upper and lower face layers by upper indices (2.3) and (2.1) respectively, whereas the values related to the core layer are denoted by (2.2). Moreover, the values related to the pre-critical stress-strain state are denoted by additional upper index 0.

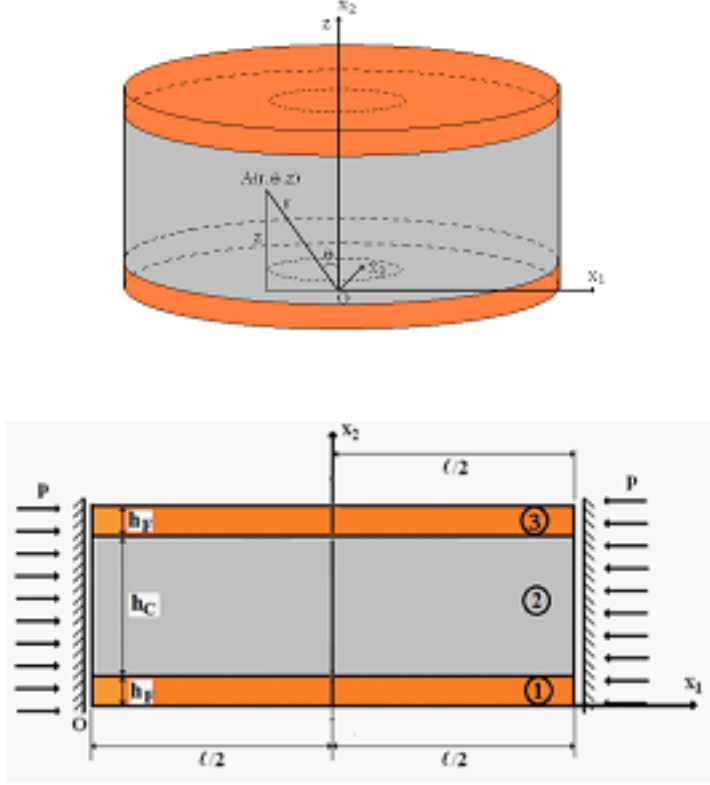


Fig. 1. The geometry of the considered circular plate (a) and the cross section of this plate with loading condition and some geometric values (b)

Within this assumptions we investigate the stability loss of the circular sandwich plate and assume that the pre-critical stress state is homogeneous and is determined according to the following expressions:

$$\sigma_{zz}^{(k),0} = 0, \sigma_{rz}^{(k),0} = 0, s_{zz}^{(k),0} = 0, D_z^{(k),0} = D_r^{(k),0} = 0, k = 1, 2, 3.$$

$$E_r^{(k),0} = a_1^{(k)} s_{rr}^{(k),0} + b_1^{(k)} s_{zz}^{(k),0}, E_z^{(k),0} = d_1^{(k)} s_{rr}^{(k),0} + c_1^{(k)} s_{zz}^{(k),0},$$

$$a_1^{(k)} = \frac{\varepsilon_{13}^{(k)} (e_{31}^{(k)} + e_{32}^{(k)}) - \varepsilon_{33}^{(k)} (e_{11}^{(k)} + e_{22}^{(k)})}{\varepsilon_{11}^{(k)} \varepsilon_{33}^{(k)} - \varepsilon_{13}^{(k)} \varepsilon_{31}^{(k)}}, b_1^{(k)} = \frac{\varepsilon_{13}^{(k)} e_{33}^{(k)} - \varepsilon_{33}^{(k)} e_{13}^{(k)}}{\varepsilon_{11}^{(k)} \varepsilon_{33}^{(k)} - \varepsilon_{13}^{(k)} \varepsilon_{31}^{(k)}},$$

$$d_1^{(k)} = \frac{\varepsilon_{11}^{(k)} (e_{31}^{(k)} + e_{32}^{(k)}) - \varepsilon_{31}^{(k)} (e_{11}^{(k)} + e_{12}^{(k)})}{\varepsilon_{13}^{(k)} \varepsilon_{31}^{(k)} - \varepsilon_{11}^{(k)} \varepsilon_{33}^{(k)}}, c_1^{(k)} = \frac{\varepsilon_{11}^{(k)} e_{33}^{(k)} - \varepsilon_{31}^{(k)} e_{13}^{(k)}}{\varepsilon_{13}^{(k)} \varepsilon_{31}^{(k)} - \varepsilon_{11}^{(k)} \varepsilon_{33}^{(k)}}.$$

$$s_{zz}^{(k),0} = a_{zr}^{(k)} s_{rr}^{(k),0}, a_{zr}^{(k)} = \frac{c_{31}^{(k)} + c_{32}^{(k)} - e_{13}^{(k)} a_1^{(k)} - e_{33}^{(k)} d_1^{(k)}}{c_{33}^{(k)} - e_{13}^{(k)} b_1^{(k)} - e_{33}^{(k)} c_1^{(k)}}.$$

$$\begin{aligned} \sigma_{rr}^{(k),0} &= A_r^{(k)} s_{rr}^{(k),0}, A_r^{(k)} = c_{11}^{(k)} + c_{12}^{(k)} - e_{11}^{(k)} a_1^{(k)} + a_{zr}^{(k)} c_{13}^{(k)} - a_{zr}^{(k)} e_{11}^{(k)} b_1^{(k)} - a_{zr}^{(k)} e_{31}^{(k)} c_1^{(k)}. \\ s_{rr}^{(1),0} &= s_{rr}^{(2),0}, 2h_f \sigma_{rr}^{(1),0} + h_C \sigma_{rr}^{(2),0} = hp, \sigma_{rr}^{(1),0} = p \left(2 \frac{h_f}{h} + \frac{h_C}{h} \frac{A_r^{(2)}}{A_r^{(1)}} \right)^{-1}. \end{aligned} \quad (2.1)$$

In (2.1) $\sigma_{rr}^{(k),0}, \dots$, and $s_{rr}^{(k),0}, \dots$, are the components of the stress and Green strain tensors, respectively, $u_r^{(k),0}$ and $u_z^{(k),0}$ are components of the displacement vector, $D_r^{(k),0}$ and $D_z^{(k),0}$ are the components of the electrical displacement vector, $E_r^{(k),0}$ and $E_z^{(k),0}$ are the components of the electric field vector, and $c_{ij}^{(k)}, e_{ij}^{(k)}$ and $\varepsilon_{nj}^{(k)}$ are the elastic, piezoelectric and dielectric constants, respectively.

Note that the expressions in (2.1) are approximate in the near vicinity of the lateral boundary surface on which the external compressional radial forces act. Nevertheless, as we will consider the cases where $h/\ell \sim 10^{-1}$ (where $h = 2h_f + h_C$ (Fig. 1), therefore the influence of the mentioned proximity on the values of the critical parameters is insignificant. Moreover, note that the expressions in (2.1) are obtained within the scope of the ‘‘open-circuit’’ condition satisfied on the face layers upper and lower plane-boundaries, according to which, the normal component of the electrical displacement vector on these planes is equal to zero.

Thus, within the scope of the foregoing assumptions, according to Guz (1999), Yang (2005), Akbarov and Yahnioglu (2013) the 3D linearized stability loss equations and relations for the case under consideration are obtained as follows:

3D linearized stability loss equations

$$\begin{aligned} \frac{\partial t_{rr}^{(k)}}{\partial r} + \frac{\partial t_{zr}^{(k)}}{\partial z} + \frac{1}{r}(t_{rr}^{(k)} - t_{\theta\theta}^{(k)}) &= 0, \frac{\partial t_{rz}^{(k)}}{\partial r} + \frac{\partial t_{zz}^{(k)}}{\partial z} + \frac{1}{r}t_{rz}^{(k)} = 0, \frac{\partial D_R^{(k)}}{\partial r} + \frac{1}{r}D_R^{(k)} + \frac{\partial D_Z^{(k)}}{\partial z} = 0. \\ t_{rr}^{(k)} &= \sigma_{rr}^{(k)} + \sigma_{rr}^{(k),0} \frac{\partial u_r^{(k)}}{\partial r} + M_{rr}^{(k)}, t_{\theta\theta}^{(k)} = \sigma_{\theta\theta}^{(k)} + \sigma_{\theta\theta}^{(k),0} \frac{u_r^{(k)}}{r} + M_{\theta\theta}^{(k)}, \\ t_{zr}^{(k)} &= \sigma_{zr}^{(k)} + M_{zr}^{(k)}, t_{rz}^{(k)} = \sigma_{rz}^{(k)} + \sigma_{rz}^{(k),0} \frac{\partial u_z^{(k)}}{\partial r} + M_{rz}^{(k)}, t_{zz}^{(k)} = \sigma_{zz}^{(k)} + M_{zz}^{(k)}, \\ M_{rr}^{(k)} &= E_r^{(k),0} E_r^{(k)} - E_\theta^{(k),0} E_\theta^{(k)} - E_z^{(k),0} E_z^{(k)}, M_{\theta\theta}^{(k)} = E_\theta^{(k),0} E_\theta^{(k)} - E_r^{(k),0} E_r^{(k)} - E_z^{(k),0} E_z^{(k)}, \\ M_{zz}^{(k)} &= E_z^{(k),0} E_z^{(k)} - E_\theta^{(k),0} E_\theta^{(k)} - E_r^{(k),0} E_r^{(k)}. \end{aligned} \quad (2.2)$$

Linearized strain-displacement relations

$$s_{rr}^{(k)} = \frac{\partial u_r^{(k)}}{\partial r}, s_{\theta\theta}^{(k)} = \frac{u_r^{(k)}}{r}, s_{zz}^{(k)} = \frac{\partial u_z^{(k)}}{\partial z}, s_{rz}^{(k)} = \frac{1}{2} \left(\frac{\partial u_r^{(k)}}{\partial z} + \frac{\partial u_z^{(k)}}{\partial r} \right), \quad (2.3)$$

Linearized electro-mechanical relations

$$\begin{aligned} \sigma_{rr}^{(k)} &= c_{11}^{(k)} s_{rr}^{(k)} + c_{12}^{(k)} s_{\theta\theta}^{(k)} + c_{13}^{(k)} s_{zz}^{(k)} - e_{11}^{(k)} E_r^{(k)} - e_{31}^{(k)} E_z^{(k)}, \\ \sigma_{\theta\theta}^{(k)} &= c_{12}^{(k)} s_{rr}^{(k)} + c_{22}^{(k)} s_{\theta\theta}^{(k)} + c_{23}^{(k)} s_{zz}^{(k)} - e_{12}^{(k)} E_r^{(k)} - e_{32}^{(k)} E_z^{(k)}, \\ \sigma_{zz}^{(k)} &= c_{31}^{(k)} s_{rr}^{(k)} + c_{32}^{(k)} s_{\theta\theta}^{(k)} + c_{33}^{(k)} s_{zz}^{(k)} - e_{13}^{(k)} E_r^{(k)} - e_{33}^{(k)} E_z^{(k)}, \\ \sigma_{rz}^{(k)} &= c_{15}^{(k)} s_{rz}^{(k)} - e_{15}^{(k)} E_r^{(k)} - e_{35}^{(k)} E_z^{(k)}, \end{aligned}$$

$$\begin{aligned}
D_r^{(k)} &= e_{11}^{(k)} s_{rr}^{(k)} + e_{12}^{(k)} s_{\theta\theta}^{(k)} + e_{13}^{(k)} s_{zz}^{(k)} + \varepsilon_{11}^{(k)} E_r^{(k)} + \varepsilon_{13}^{(k)} E_z^{(k)}, \\
D_z^{(k)} &= e_{31}^{(k)} s_{rr}^{(k)} + e_{32}^{(k)} s_{\theta\theta}^{(k)} + e_{33}^{(k)} s_{zz}^{(k)} + \varepsilon_{31}^{(k)} E_r^{(k)} + \varepsilon_{33}^{(k)} E_z^{(k)}, \\
E_r^{(k)} &= -\frac{\partial\phi^{(k)}}{\partial r}, E_z^{(k)} = -\frac{\partial\phi^{(k)}}{\partial z}.
\end{aligned} \tag{2.4}$$

where $\phi^{(k)}$ is an electric potential for the k - th layer material

Note that the relations in (2.1) - (2.4) are written for the piezoelectric materials and supposing that $e_{ij}^{(k)} = 0$ and $\varepsilon_{ij}^{(k)} = 0$ we can obtain the mechanical relations for the elastic materials. Moreover, note that under writing of the relations in (2.4) it is assumed that the polled direction of the piezoelectric material is the Oz axis direction (Fig. 1). At the same time, we assume that the contact and boundary conditions given below satisfy.

$$\begin{aligned}
t_{zz}^{(3)} \Big|_{z=h_F+h_C} &= t_{zz}^{(2)} \Big|_{z=h_F+h_C}, \\
t_{zr}^{(3)} \Big|_{z=h_F+h_C} &= t_{zr}^{(2)} \Big|_{z=h_F+h_C}, u_z^{(3)} \Big|_{z=h_F+h_C} = u_z^{(2)} \Big|_{z=h_F+h_C}, \\
u_r^{(3)} \Big|_{z=h_F+h_C} &= u_r^{(2)} \Big|_{z=h_F+h_C}, t_{zz}^{(2)} \Big|_{z=h_F} = t_{zz}^{(1)} \Big|_{z=h_F}, t_{zr}^{(2)} \Big|_{z=h_F} = t_{zr}^{(1)} \Big|_{z=h_F}, \\
u_z^{(2)} \Big|_{z=h_F} &= u_z^{(1)} \Big|_{z=h_F}, u_r^{(2)} \Big|_{z=h_F} = u_r^{(1)} \Big|_{z=h_F}, \\
t_{zz}^{(2,3)} \Big|_{z=2h_F+h_C} &= 0, t_{zr}^{(2,3)} \Big|_{z=2h_F+h_C} = 0, t_{zz}^{(2,1)} \Big|_{z=0} = 0, t_{zr}^{(2,1)} \Big|_{z=0} = 0 \text{ for } 0 \leq r \leq \ell/2, \\
t_{rr}^{(k)} \Big|_{r=\ell/2} &= 0, u_z^{(k)} \Big|_{r=\ell/2} = 0, \text{ for } k = 1, 2, 3 \text{ under } r = \ell/20 \leq z \leq 2h_F + h_C.
\end{aligned} \tag{2.5}$$

Note that the conditions given in (5) relate to the mechanical quantities and the corresponding conditions for the electrical quantities are given for the components of the electrical displacements $D_z^{(k)}$ and $D_r^{(k)}$, or for the electric potential $\phi^{(k)}$. In the present investigation we assume that

$$D_z^{(3)} \Big|_{z=2h_F+h_C} = 0, D_z^{(3)} \Big|_{z=h_F+h_C} = 0, D_z^{(1)} \Big|_{z=0} = 0, D_z^{(1)} \Big|_{z=h_F} = 0, \tag{2.6}$$

$$\phi^{(3)} \Big|_{r=\ell/2} = 0, \phi^{(1)} \Big|_{r=\ell/2} = 0. \tag{2.7}$$

Note that in the theory of piezoelectricity the conditions in (2.6) are called the ‘‘open-circuit’’, however the conditions in (2.7) the ‘‘short-circuit’’ ones. Consequently, in the present investigation we assume that on the face planes of the piezoelectric layers the ‘‘open-circuit’’, however on the lateral cylindrical surfaces of those the ‘‘short-circuit’’ conditions are satisfied.

This completes the formulation of the problem, according to which, the determination of the critical values of the pre-critical quantities is reduced to the solution of the eigenvalue problem (2.2) - (2.7).

3 FEM modelling of the problem.

We attempt to solve to the problem formulated in the previous section by employing FEM and for this purpose, according to Guz (1999), Yang (2005), Akbarov (2013) and others, we introduce the following functional.

$$\begin{aligned}
& \Pi(u_r^{(1)}, u_r^{(2)}, u_r^{(3)}, u_z^{(1)}, u_z^{(2)}, u_z^{(3)}, \phi^{(1)}, \phi^{(2)}, \phi^{(3)}) \\
&= \frac{1}{2} \sum_{k=1}^3 \iint_{\Omega^{(k)}} \left[t_{rr}^{(k)} \frac{\partial u_r^{(k)}}{\partial r} + t_{\theta\theta}^{(k)} \frac{u_r^{(k)}}{r} + t_{rz}^{(k)} \frac{\partial u_z^{(k)}}{\partial r} + t_{zr}^{(k)} \frac{\partial u_r^{(k)}}{\partial z} \right. \\
&\quad \left. + t_{zz}^{(k)} \frac{\partial u_z^{(k)}}{\partial z} + E_r^{(k)} D_r^{(k)} + E_z^{(k)} D_z^{(k)} \right] r dr dz, \tag{3.1}
\end{aligned}$$

where

$$\Omega^{(1)} = \{0 \leq r \leq \ell/2; 0 \leq z \leq h_F\}, \Omega^{(2)} = \{0 \leq r \leq \ell/2; h_F \leq z \leq h_F + h_C\},$$

$$\Omega^{(3)} = \{0 \leq r \leq \ell/2; h_F + h_C \leq z \leq 2h_F + h_C\}. \tag{3.2}$$

From equating to zero the first variation of the functional (2.7), i.e. from the relation

$$\delta \Pi = \sum_{k=1}^3 \frac{\partial \Pi}{\partial u_r^{(k)}} \delta u_r^{(k)} + \sum_{k=1}^3 \frac{\partial \Pi}{\partial u_z^{(k)}} \delta u_z^{(k)} + \sum_{k=1}^3 \frac{\partial \Pi}{\partial \phi^{(k)}} \delta \phi^{(k)} = 0, \tag{3.3}$$

and after well-known mathematical manipulations we obtain the first three equations in (2.2). The boundary and contact conditions in (2.5) - (2.7) are given with respect to the forces and electrical displacements. In this way it is proven that the first three equations in (2.2) are the Euler equations for the functional (3.1) and the boundary and contact conditions in (2.5) - (2.7) which are given with respect to the forces and electrical displacements, are the related natural boundary and contact conditions.

According to FEM modelling, the solution domains indicated in (3.1) are divided into a finite number of finite elements. For the considered problem each of the finite elements is selected as a standard rectangular Lagrange family quadratic finite element (i.e. with nine nodes) and each node has three degrees of freedom, i.e. radial displacement $u_r^{(k)}$, transverse displacement $u_z^{(k)}$ and electric potential $\phi^{(k)}$. Employing the standard Ritz technique detailed in many references, for instance, in the book by Zienkiewicz and Taylor (1989), we determine the displacements and electrical potential at the selected nodes. After this determination, from the equation

$$\det(K) = 0 \tag{3.4}$$

the values of the critical compressional forces are determined, where K is a corresponding stiffness matrix. The solution procedure of the equation (3.4) is made according to the well-known "bi-section" method which basis on the sign change of the $\det(K)$.

This completes the consideration of the method of solution.

4 Numerical results and discussions.

Note that in the present paper, the piezoelectric materials PZT -5H, PZT -4 and BaTiO₃ are taken as the face layer materials, however the metal materials - aluminum (Al) and steel(St) are taken as the core layer materials. The values of the elastic, piezoelectric and dielectric constants of the selected piezoelectric materials and the references used are given in Table 1.

Table 1. The values of the mechanical, piezoelectrical and dielectrical constants of the selected piezoelectric materials

Materials (Source Ref.)	$c_{11}^{(r_1)}$	$c_{12}^{(r_1)}$	$c_{13}^{(r_1)}$	$c_{33}^{(r_1)}$	$c_{44}^{(r_1)}$	$c_{66}^{(r_1)}$	$e_{31}^{(r_1)}$	$e_{33}^{(r_1)}$	$e_{15}^{(r_1)}$	$\varepsilon_{11}^{(r_1)}$	$\varepsilon_{33}^{(r_1)}$
PZT-4 (Yang, 2005))	13.9	7.78	7.40	11.15	2.56	3.06	-5.2	15.1	12.7	0.646	0.562
PZT-5H (Yang, 2005))	12.6	7.91	8.39	11.7	2.30	2.35	-6.5	23.3	17.0	1.505	1.302
BaTiO ₃ (Kuna, 2006)	16.6	7.66	7.75	16.2	4.29	4.29	-4.4	18.6	11.6	1.434	1682
	$\times 10^{10} N/m^2$						C/m^2			$\times 10^{-8} C/Vm$	

According to Guz (2004), the values of Lamé's constants of the core layer material is selected as follows: for the Al: $\lambda = 48.1 GPa$ and $\mu = 27.1 GPa$; for the St: $\lambda = 92.6 GPa$ and $\mu = 77.5 GPa$.

Under FEM modelling using the symmetry with respect to the plane $z = h_F + h_C/2$ and the axial symmetry with respect to the Oz (Fig. 1a) axis of the mechanical and geometrical properties of the plate, we consider only the region $\{0 \leq r \leq \ell/2; 0 \leq z \leq h_F + h_C\}$ and this region is divided into 40 finite elements along the radial direction and 12 finite elements along the plate's thickness direction, resulting in 31022 NDOF. Such selection of the finite elements numbers is established according to the convergence of the numerical results. All the corresponding PC programs are composed by the authors of the paper.

Table 2. The values of the critical stresses σ_{cr}^{21} , σ_{cr}^{22} and \bar{p}_{cr} obtained for the case where the material of the core layer is steel in the cases where the piezoelectric constants of PZT are equated to zero (upper number), and are equal to the corresponding data given in Table 1 (lower number)

h_F/ℓ	Crit.Param.	Materials of the face layers		
		PZT-5H	PZT-4	BaTiO ₃
1/40	σ_{cr}^{10}	0.1015	0.1399	0.1249
	$\sigma_{cr}^{(1)}$	0.1925	0.2244	0.1418
	$\sigma_{cr}^{(2)}$	0.3246	0.3120	0.2010
	\bar{p}_{cr}	0.3578	0.3375	0.2053
1/30	$\sigma_{cr}^{(1)}$	0.2689	0.2690	0.1820
	$\sigma_{cr}^{(2)}$	0.3165	0.3093	0.1895
	$\sigma_{cr}^{(1)}$	0.0946	0.1337	0.1222
	$\sigma_{cr}^{(2)}$	0.1858	0.2194	0.1394
1/24	$\sigma_{cr}^{(1)}$	0.3026	0.2982	0.1965
	$\sigma_{cr}^{(2)}$	0.3453	0.3302	0.2019
	\bar{p}_{cr}	0.2333	0.2434	0.1718
	\bar{p}_{cr}	0.2922	0.2933	0.1811
1/20	$\sigma_{cr}^{(1)}$	0.0896	0.1296	0.1206
	$\sigma_{cr}^{(2)}$	0.1816	0.2165	0.1381
	$\sigma_{cr}^{(1)}$	0.2866	0.2888	0.1940
	$\sigma_{cr}^{(2)}$	0.3377	0.3258	0.2000
1/20	\bar{p}_{cr}	0.2046	0.2225	0.1635
	\bar{p}_{cr}	0.2727	0.2803	0.1743
	$\sigma_{cr}^{(1)}$	0.0867	0.1274	0.1202
	$\sigma_{cr}^{(2)}$	0.1800	0.2156	0.1379
1/20	$\sigma_{cr}^{(1)}$	0.2774	0.2841	0.1933
	$\sigma_{cr}^{(2)}$	0.3345	0.3243	0.1998
	\bar{p}_{cr}	0.1821	0.2058	0.1568
	\bar{p}_{cr}	0.2573	0.2700	0.1689

The algorithm and programs employed in the present investigations are some modifications and development of the corresponding algorithm and programs used and testing in the many investigations and discussed in the monograph by Akbarov (2013). Consequently, the validity and trustiness of the used in the present investigations PC programs and algorithm cause no doubt.

For simplification of the consideration, we introduce the following notation for the dimensionless critical radial stresses and critical compressive forces:

$$\sigma_{cr}^{(1)} = \sigma_{rr.cr}^{(1),0} / c_{44}^{(1)}, \sigma_{cr}^{(2)} = \sigma_{rr.cr}^{(2),0} / c_{44}^{(1)}, \bar{p}_{cr} = p / c_{44}^{(1)}. \quad (4.1)$$

Thus, according to (4.1), we estimate the work carrying capacity of the plate under consideration with respect to the stability loss by simultaneous use of the values of three dimensionless critical parameters which are the dimensionless radial compressive stress $\sigma_{cr}^{(2,1)}$ in the face piezoelectric layer, the dimensionless radial compressive stress $\sigma_{cr}^{(2,2)}$ in the core metal layer and the dimensionless intensity \bar{p}_{cr} of the external compressive force. Such an approach for estimation of the buckling delamination allows us to have more precise information on the influence of the problem parameters such as the piezoelectricity of the face layers' materials, the face layers' thickness and the mechanical properties of the layers' materials.

Thus, we consider the numerical results obtained for the critical parameters indicated in (4.1) and detailed above. Note that these results are given in Tables 2 and 3 which are obtained for the cases where the material of the core layer is St and Al respectively. Moreover, note that these results are obtained for the cases where face layers materials are PZT-5H, PZT-4 and BaTiO₃. For estimation of the influence of the face layers' piezoelectricity on the values of the critical stresses in the tables, two types of results are presented simultaneously, the first of which (upper number) relates to the case where the values of the piezoelectric and dielectric constants of the face layer materials are equated to zero, i.e. coupling of the mechanical and electrical fields is not taken into consideration. However, under obtaining the second type of results (lower number) the values of the piezoelectric and dielectric constants are taken into consideration as given in Table 1 and the coupling effect between the electrical and mechanical fields is taken into consideration completely.

Table 3. The values of the critical dimensionless stresses $\sigma_{cr}^{(2,1)}$, $\sigma_{cr}^{(2,2)}$ and \bar{p}_{cr} obtained for the case where the material of the core layer is aluminum in the cases where the piezoelectric constants of PZT are equated to zero (upper number), and are equal to the corresponding data given in Table 1 (lower number)

h_F/ℓ	Crit.Param.	Materials of the face layers		
		PZT-5H	PZT-4	BaTiO ₃
1/40	σ_{cr}^1	0.1264 0.2430 0.1491	0.1772 0.2828 0.1458	0.1586 0.1793 0.0941
	σ_{cr}^I	0.1667 0.1435	0.1570 0.1537	0.0958 0.1103
	\bar{p}_{cr}	0.1858	0.1884	0.1167
	$\sigma_{cr}^{(1)}$	0.1259 0.2434	0.1777 0.2823	0.1590 0.1792
1/30	$\sigma_{cr}^{(2)}$	0.1485 0.1670 0.1410	0.1461 0.1567 0.1567	0.0944 0.0957 0.1160
	\bar{p}_{cr}	0.1925	0.1986	0.1236
	$\sigma_{cr}^{(1)}$	0.1259 0.2422	0.1773 0.2795	0.1580 0.1775
	$\sigma_{cr}^{(2)}$	0.1485 0.1662 0.1391	0.1458 0.1552 0.1590	0.0938 0.0948 0.1206
1/24	\bar{p}_{cr}	0.1979 0.1261	0.2070 0.1762	0.1293 0.1559
	σ_{cr}^1	0.2402 0.1488	0.2750 0.1449	0.1746 0.0926
	σ_{cr}^I	0.1647 0.1375	0.1527 0.1606	0.0933 0.1243
	\bar{p}_{cr}	0.2205	0.2139	0.1340

Analysis of the results shows that for all the cases under consideration the piezoelectricity of the face layers causes an increase in the values of the dimensionless critical stresses $\sigma_{cr}^{(2,1)}$, $\sigma_{cr}^{(2,2)}$ and \bar{p}_{cr} . However this increase is more significant for the PZT-5H and PZT-4 than that for the BaTiO₃.

The discussed above character of the influence of the piezoelectricity of the face layers materials on the values of the dimensionless critical stresses can be explained with the so-called "piezoelectric stiffening" effect of the piezoelectric materials, i.e. with the increase of the material stiffness as a result of the piezoelectricity of that. Consequently, the fact that an increase of the thickness of the face layers also increases the stiffness of the piezoelectric layers. However, under fixed h/ℓ ($=0.2$) thickness of the plate an increase h_F/ℓ causes a decrease of the h_C/ℓ as a result of which the whole stiffness of the plate depends on the ratio of stiffnesses of the core and face layers materials. Under explanation of the results discussed above it is also necessary to take into consideration of the complicate character of the dependence between the selected dimensionless critical stress and the ratio of the stiffnesses of the layers.

Namely with the foregoing statements it can be explained the character of the influence of the change h_F/ℓ on the values of the critical stresses. According to the results given in Tables 2 and 3 this character can be formulated as follows:

- 1 For the pairs of materials consisting of PZT + St an increase in the values of h_F/ℓ causes to decrease in all the values of the critical stresses under consideration;
- 2 For the pairs of materials consisting of PZT + Al the values of \bar{p}_{cr} increase with h_F/ℓ , however dependence among $\sigma_{cr}^{(1)}$, $\sigma_{cr}^{(2)}$ and h_F/ℓ has non-monotonic character.

This completes the discussions of the obtained numerical results.

5 Conclusion.

Thus, in the present paper within the scope of the three-dimensional linearized theory of stability for piezoelectric materials, the axisymmetric stability loss of the PZT/Metal/PZT sandwich circular plate has been investigated. The case where "open-circuit" conditions with respect to the electrical displacement on the upper and lower surfaces, and short-circuit conditions with respect to the electrical potential on the lateral surface of the face layers are satisfied, is considered. The corresponding eigenvalue problem is solved numerically by employing FEM. Numerical results are presented in Tables 2 and 3 for the PZT-5H/Al/PZT-5H, PZT-4/Al/PZT-4, BaTiO₃/Al/BaTiO₃, PZT-5H/St/PZT-5H, PZT-4/St/PZT-4 and BaTiO₃/St/ BaTiO₃ plates, respectively. These results illustrate simultaneously the values of the critical dimensionless radial compressive stress $\sigma_{cr}^{(1)}$ acting in the face piezoelectric layer, the values of the dimensionless critical compressive radial stress $\sigma_{cr}^{(2)}$ acting in the core-metal layer and the values of the dimensionless critical stress of the intensity \bar{p}_{cr} of the external compressive forces obtained in the case where the piezoelectricity, i.e. the coupling effect, are taken into consideration (lower number in the tables) and in the case where the coupling effect is not taken into consideration (upper number in the tables). According to these results, the concrete conclusions on the influence of the electro-mechanical and geometrical parameters of the sandwich circular plate under consideration on the values of the dimensionless stresses are made. Note that these conclusions are formulated in the text of the previous section.

We recall that the discussed above results are obtained within the scope of the "open-circuit" conditions on the upper and lower face planes of the piezoelectric layers in the case where the polled direction of that is the Oz axis direction. However, there are also many

cases where the conditions on the face planes of the piezoelectric layers are "short-circuit" ones satisfy and the polled direction of the piezoelectric material coincides with the radial direction shown in Fig. 1. The corresponding investigations related to these latter cases will be considered in further works by the authors.

References

1. Akbarov, S.D.: Stability Loss and Buckling Delamination: Three-Dimensional Linearized Approach for Elastic and Viscoelastic Composites. *Springer, Heidelberg, New York* (2013).
2. Akbarov, S.D., Yahnioglu, N.: *Buckling delamination of a sandwich plate-strip with piezoelectric face and elastic core layers*, *Appl. Math. Model.* **37**, 8029 - 8038 (2013).
3. Akbarov, S.D., Rzayev, O.G.: *On the buckling of the elastic and viscoelastic composite circular thick plate with a penny-shaped crack*. *Eur. J Mech. A Solid.* **21** (2), 269–279 (2002).
4. Wu, C.P., Ding, S.: *Coupled electro-elastic analysis of functionally graded piezoelectric material plates*. *Smart Structures and Systems*, **16** (5) 781 – 806 (2015).
5. Arefi, M., Allam, M.N.M.: *Nonlinear responses of an arbitrary FGP circular plate resting on the Winkler - Pasternak foundation*. *Smart Structures and Systems*, **16** (1), 81 – 100 (2015).
6. Guz, A.N.: *Fundamentals of the Three-Dimensional Theory of Stability of Deformable Bodies*. *Springer-Verlag, Berlin Heidelberg* (1999).
7. Guz, A.N.: *Elastic waves in bodies with initial (residual) stresses*. *A.C.K., Kiev* (2004).
8. Jabbari, M., Farzaneh, Joubaneh, E., Khorshidvand, A.R., Eslami, M.R.: *Buckling analysis of porous circular plate with piezoelectric actuator layers under uniform radial compression*. *Int. J. Mech. Science.* **70**, 50–56 (2013).
9. Kuna, M.: *Finite element analysis of cracks in piezoelectric structures: a survey*. *Arch. Appl. Mech.* **76**, 725–745 (2006).
10. Rzayev, O.G., Akbarov, S.D.: *Local buckling of the elastic and viscoelastic coating around the penny-shaped interface crack*. *Int. J Eng. Sci.* **40**, 1435–1451 (2002).
11. Yang, J.S.: *Buckling of a piezoelectric plate*. *Int. J. Appl. Electromagn. Mech.* **9**, 399–408 (1998).
12. Yang, J.S.: *An introduction to the theory of piezoelectricity*. *Springer, New-York* (2005).
13. Zienkiewicz, O.C., Taylor, R.L.: *Basic formulation and linear problems. The finite element method, 4-th edn. McGraw-Hill, New York*, **1**, (1989).